Author's response GMDD-2015-82

The author wishes to thank the editor and reviewers for identifying corrections in the coding and improvements to the text. As noted in an earlier response, the Cloud-J code is now revised and available as version 7.3c. There was confusion over the use of "correlation" and whether that implied statistics. The text has been revised to be more consistent and to use the more typical term 'decorrelation length' while keeping 'cc' as the 'cloud correlation factor'.

Specific responses to Editor

The historic naming of the Fast-J codes has been clarified in the text and in a readme file on the ftp site. The changing of names sounded like a good idea at the time, but version numbers would have proven better.

Specific responses to Review 1

Why 4 QCAs yields only 2.8 calls on average to Fast-J is explained in the text where that number is first used, but not the abstract as that would be too cumbersome. The simple explanation is that QCAs use 4 specific optical depth ranges and not all fractional-cloudy atmospheres have all 4 cloud types of the QCA.

The explanation of vertical correlation of clouds and their decorrelation length over which they become randomly overlapped is expanded. While the determination of the decorrelation lengths (see referenced papers) is statistical, their use in Cloud-J is deterministic: (i) the length defines the MAX groupings, and (ii) the correlation factor between the MAX groupings (0.33) is chosen to be intermediate, about an e-fold, between random overlap (0.00) and maximum overlap (1.00). Horizontal correlations are not considered and that should be clear from the derivations. With Fast-J and Cloud-J the calculation centers on a vertical column atmosphere. Thus resolution independence is with respect to the number of vertical layers. The paper notes that number of MAX groups is fixed by altitude and hence is resolution independent. Further, by binning the cloud fraction into a fixed resolution, the number of independent column atmospheres (ICAs) in any MAX group does not depend on the number of layers. For example 10% bins in cloud fraction are used here, leading to a maximum of 10 ICAs in any MAX group.

In revising the section on decorrelation, it became clear that the v7.3 code did not reduce the correlation of overlapping MAX-COR cloud groups when they were separated by a gap (i.e., an extra decorrelation length). This has been corrected with v7.3c. The numbers generated for the Cloud-J evaluation here (many more than shown) changed by at most 0.1% and are not discernible in the GMDD figures and tables.

The function 'modulo' has been expanded from programmer language (mod) to English (thanks).

As noted above and in the revised text, the choice of cc = 0.33 is logical based on the decorrelation length and does not depend on model resolution.

The coding re TITCLD (and similar anomalies) has been corrected (thanks for catching this).

Specific responses to Review 2

1) The correlation coefficient was incorrect usage and the manuscript is revised as noted above. The definition of cc is now justified, as is the recommendation of G6/.33 as the best physically based model for cloud overlap.

$$g^{L1} = 1 + cc * (1/f^{L2} - 1)$$

The derivation of this has several approaches: The RAN ICAs have a weight assigned to the L1-cloud layer that does not depend on the layer above. Hence, the L1-cloud under the L2-cloud (i.e., the cloudy-cloudy ICA) has a fractional area of f1*f2 and that of the L1 cloud under the L2 clear sky is f1*(1-f2). With MAX overlap, the fractional area with L1-cloud and L2-cloud is just f1 (i.e., the largest fractional area that can have clouds in L1 and L2. With MAX there is no L1-cloud under clear sky. (This example assumes that f1 < f2, but the alternate case can be readily assigned in a similar way.) So the purpose of the factor g is to interpolate linearly for the weight of cloud-L1 below cloud-L2 from a value of f1 to 1. The factor g increases linearly between 1 and 1/f2 as cc increases, meeting the requirement that the weight of the cloudy-cloudy ICA increase from f2*f1*g = f1*f2 to f1 as required. This form of *g1* is thus the one and only linear function in cc interpolating function between the two limits.

2.) This is an interesting question (consistency of solar flux calculations in terms of global radiative budget under different cloud fraction assumptions), but beyond this researcher. Validation of code with 3D requires one to specific the horizontal spatial correlations, and it is those that will determine agreement between a plane-parallel and 3D approach. Again, an interesting question, but the data just does not come from typical climate or even high-resolution forecast models.

3.) Apologies, all the atmospheres (from all longitudes) were used with a single solar zenith angle (13.6°) and surface albedo (0.10). This is now noted in the figure caption.

4) Thanks for the pointers. A careful re-read of the text found some additional verb tense problems and these are now fixed. Other wording suggestions are now adopted.

5) The figure has been fixed so that the ‘f’ notations matches the equations – it was from an earlier draft.

\documentclass[gmdd, online, hvmath]{copernicus}

\begin{document}\hack{\sloppy}

\title{Photolysis rates in correlated overlapping cloud fields: Cloud-J~7.3}

\Author{M.~J.}{Prather}

\affil{Earth System Science Department, UC Irvine California, USA}

\correspondence{M.~J.~Prather (mprather@uci.edu)}

\runningtitle{Photolysis rates in correlated overlapping cloud fields: Cloud-J~7.3}

\runningauthor{M.~J. Prather}

\received{29~April~2015}
\accepted{6~May~2015}
\published{}

\firstpage{1}

\maketitle

\begin{abstract}
A~new approach for modeling photolysis rates (J~values) in atmospheres
with fractional cloud cover has been developed and is implemented as
Cloud-J -- a~multi-scattering eight-stream radiative transfer model
for solar radiation based on Fast-J. Using observations of ~~ed statistics for~~
the
vertical correlation of cloud layers, Cloud-J 7.3 provides a~practical
and accurate method for modeling atmospheric chemistry. The
combination of the new maximum-correlated cloud groups with the
integration over all cloud combinations ~~represented~~ by four quadrature
atmospheres produces mean J~values in an atmospheric column with
root-mean-square errors of 4\,{\%} or less compared with 10--20\,{\%}
errors using simpler approximations. Cloud-J is practical for
chemistry-climate models, requiring only an average of 2.8 Fast-J
calls per atmosphere, vs. hundreds of calls with the correlated cloud
groups, or 1 call with the simplest cloud approximations. Another
improvement in modeling J~values, the treatment of volatile organic
compounds with pressure-dependent cross sections is also incorporated
into Cloud-J.
\end{abstract}

\introduction

Photolysis, the dissociation of molecules upon absorbing sunlight,
drives atmospheric chemistry and controls the composition of the air
we breathe. Photolysis rates are governed by the intensity and
spectral distribution of
sunlight, which is altered by scattering and absorption processes
within the atmosphere. Clouds, aerosols, and gases control these
processes; but ambiguity in the representation of clouds in
atmospheric models is currently the largest source of uncertainty in
photolysis rates. This paper presents a~new, pragmatic approach for
representing the overlap of clouds derived from observations and cloud
models, and then provides several practical approximations with

marginal computational costs that can be readily incorporated in atmospheric chemistry models. This computer code is a~major expansion of Fast-J (Wild et~al., 2000; Bian and Prather, 2002; Neu et~al., 2007) and is presented here as Cloud-J version 7.3.
(Cloud-J contains Fast-J
and thus continues that numbering sequence,
for which Fast-J 7.2 was
the last released version.
Fast-J has gone through several variants:
Fast-J began with 7 bands, full scattering, for the troposphere;
Fast-J2 added 11 bands, absorption only, for the stratosphere;
Fast-JX applied full scattering to all 18 bands.
Fast-J is used here throughout, although
some recent code versions use the JX notation.)

Clouds can increase photolysis rates through scattered sunlight, but they can greatly reduce them by shadowing. Modeling the scattering by cloud layers in a~column atmosphere and resulting photolysis rates is practical, as in Fast-J, if the layers are horizontally uniform across the modeled air parcel (defined typically as a~rectilinear box bounded by latitude, longitude and pressure surfaces). Clouds layers, however, have horizontal scales of a~few kilometers (Slobodda et~al., 2015), and thus are represented in global and regional models as fractional coverage in each parcel. In calculating the average photolysis or heating rates through the column atmosphere, one must know how the cloud fractions overlap. Early modeling assumed that model layers consisted of maximally overlapped groups (MAX) that werewould be randomly overlapped relative to one another (MAX-RAN) (Briegleb, 1992; Feng et~al., 2004). A~more accurate description of cloud overlap is that clouds are highly correlated (i.e., maximally overlapped) when they are vertically near each other, but they become randomly overlapped when separated by greater distances. The cloud decorrelation length is the vertical distance over which the overlap e-folds to random. From a range of observations and cloud models, we estimate a~cloud des are correlated throughout the column atmosphere with a~correlation length ranging increasing from 1.5~km for the boundary layer to 3~\,\unit{km} in in the upper tropospheheight (Pincus et~al., 2005; Naud and DelGenio, 2006; Kato et~al., 2010; Oreopoulis et~al., 2012).

A~practical application of this cloud overlap information, merging maximally overlapped groups that are correlated with each other (MAX-COR), is defined in Sect.~2, where the impact of cloud overlap models on photolysis rates (J~values) is also shown. Cloud overlap models generate statistics that lead to a~large number of weighted independent column atmospheres (ICAs), where the number is too large to be used directly to calculate photolysis or heating rates in global models. Section~3 looks at the simplifiede cloud models and the approaches to approximate the sum over ICAs, examining their errors. Another recent development in modeling photolysis rates included with Cloud-J is the treatment of volatile organic compounds with pressure-dependent cross sections, presented in Sect.~4. Recommendations for the cloud-overlap model and the ICA-approximation method are discussed in Sect.~5.

\section{Overlap models for fractionally cloudy atmospheres}%s2

Typically, meteorological forecasts or climate model datas used in atmospheric chemistry models report fractionally cloudy atmospheres (FCAs) in each grid-square. Computation of the photolysis or heating rates in an FCA requires knowledge of how the clouds in each layer

overlap. The calculation of J~values in most atmospheric chemistry models today involves solving the radiative transfer equations in a~plane-parallel atmosphere where the vertical layers can be highly inhomogeneous but the horizontal planes are uniform (Stamnes et~al., 1988; Wild et~al., 2000; Tie et~al., 2003). Thus, the only workable method (other than 3-D radiative transfer) is to represent the FCA by a~number of independent column atmospheres (ICAs) where each ICA is either 100\,{\%} cloudy or clear in each layer. The fractional cloud overlap model determines the layer-structure, weighting, and number of ICAs. Other simple cloud models approximate~~d~~ overlap by: (i)~ignoring clouds entirely (clear sky), (ii)~averaging the cloud fraction~~al cloud~~, f, over each layer, conserving total cloud water (average clouds); and (iii)~~~in~~decreasing the cloud fraction and cloud water in a layer by using a reduced cloud fraction, $f^{3/2}$ followed by averaging across the layer ~~, increasing the~~
~~total cloud water in proportion, and then averaging over the layer~~
(Briegleb, 1992). These methods ~~will~~ are~~be~~ compared with cloud overlap models in Sect.~3. Here, we focus on how the ICAs differ across cloud overlap models.

\subsection{Random overlap (RAN)}%s2.1

The ways in which fractionally cloudy layers can overlap is shown schematically in Fig.~1. One assumption is random overlap (RAN). In this case the likelihood (fractional weight, w) of having the cloud in layer L1 fall below the cloud in layer L2 is random and hence equals $f^{\mathrm{L}1}$. This particular pairing -- cloud below cloud -- becomes ICA {\#}1. Superscripts in the equations below refer to atmospheric layers. The likelihood for the clear layer under the cloudy layer is by default the complement.
\begin{align}
&w^{\mathrm{L}1} ({\#}1) = f^{\mathrm{L}1}\\
%
&w^{\mathrm{L}1} ({\#}2) = 1-f^{\mathrm{L}1}
\end{align}%e1 e2
The likelihood of the cloudy layer in L2 above is
\begin{align}
&w^{\mathrm{L}2} ({\#}1) = w^{\mathrm{L}2} ({\#}2) = f^{\mathrm{L}2}
\end{align}%e3
The total weight W for each ICA {\#}1 and {\#}2 is then the product of $w^{\mathrm{L}1}$ and $w^{\mathrm{L}2}$.
\begin{align}
&W^{\mathrm{L}1-\mathrm{L}2} ({\#}1) = w^{\mathrm{L}1} ({\#}1) w^{\mathrm{L}2} ({\#}1) = f^{\mathrm{L}1} f^{\mathrm{L}2} = 0.15 \times 0.20 = 3\,{\%}~(\text{from Fig.~1})\\
%
&W^{\mathrm{L}1-\mathrm{L}2} ({\#}2) = w^{\mathrm{L}1} ({\#}2) w^{\mathrm{L}2} ({\#}2) = (1-f^{\mathrm{L}1}) f^{\mathrm{L}2} = 0.85 \times 0.20 = 17\,{\%}
\end{align}%e4 e5
Similar rules apply to ICAs {\#}3 and {\#}4,
\begin{align}
&w^{\mathrm{L}1} ({\#}3) = f^{\mathrm{L}1} \quad \text{and} \quad w^{\mathrm{L}2} ({\#}3) = 1 - f^{\mathrm{L}2}\\
%
&w^{L1} ({\#}4) = 1-f^{\mathrm{L}1} \quad \text{and} \quad w^{\mathrm{L}2} ({\#}4) = 1-f^{\mathrm{L}2}.
\end{align}%e6 e7
and thus
\begin{align}

&W^{\mathrm{L}1-\mathrm{L}2} ({\#}3) = w^{\mathrm{L}1} ({\#}3) w^{\mathrm{L}2}
({\#}3) = f^{\mathrm{L}1} (1-f^{\mathrm{L}2}) = 0.15 \times 0.80 =
12\,{\%}~(\text{Fig.~1})\\
%
&W^{\mathrm{L}1-\mathrm{L}2} ({\#}4) = w^{\mathrm{L}1} ({\#}4) w^{\mathrm{L}2}
({\#}4) = (1-f^{\mathrm{L}1}) (1-f^{\mathrm{L}2}) = 0.85 \times 0.80 = 68\,{\%}
\end{align}%e8 e9
ICAs {\#}1 and {\#}3 are tagged as cloudy in L1, and ICAs {\#}2 and
{\#}4 are tagged as clear in L1. The sum of cloudy fractions in L1
must be conserved:
3\,{\%}\,$+$\,12\,{\%}\,$=$\,15\,{\%}\,$=$\,$f^{\mathrm{L}1}$. One of
the problems in implementing a~full RAN model is that the number of
ICAs scales as 2$^{\text{NL}}$, where NL is the number of cloudy
layers in the RAN group.

\subsection{Correlated overlap (COR)}%s2.2

When correlated, the likelihood of a~cloudy layer ~~under~~lying under a ~~another~~
cloud
above is greater than random, $w^{\mathrm{L}1}$({\#}1) $>$
$f^{\mathrm{L}1}$, by a~factor $g^{\mathrm{L}1}>1$. The cloud correlation
factor ~~coefficient~~ {cc}
ranges from~0 (random) to~1 (maximal overlap).
\begin{align}
&g^{\mathrm{L}1}=1 +~\text{cc} (1/f^{\mathrm{L}2}-1),~\text{subject
to}~g^{\mathrm{L}1}\le 1/f^{\mathrm{L}1}~\text{and}~g^{\mathrm{L}1}\le
1/f^{\mathrm{L}2}
\end{align}%e10
Hence for $\text{cc}>0$ we have increased likelihood of the cloud in
L1 falling underneath the cloud in L2. For the example in Fig.~1,
$\text{cc}=0.5~~1/2~~$ and $g^{\mathrm{L}1}=3$.
\begin{align}
&w^{\mathrm{L}1} ({\#}1) = g^{\mathrm{L}1} f^{\mathrm{L}1}= 3 \times 0.15 =
45\,{\%}\\
%
&w^{\mathrm{L}1} ({\#}2) = 1-g^{\mathrm{L}1} f^{\mathrm{L}1}= 1 - 0.45 = 55\,{\%}
\end{align}%e11 e12
The likelihood of clouds in L1 falling below the clear section in L2
~~are~~ is reduced and is calculated from the requirement that the sum of cloudy
fractions in L1 is still $f^{\mathrm{L}1}$.
\begin{align}
&w^{\mathrm{L}1} ({\#}3) = f^{\mathrm{L}1} (1-g^{\mathrm{L}1} f^{\mathrm{L}2})/(1-
f^{\mathrm{L}2}) = 0.15 \times (1 - 3 \times 0.20)/0.80 = 7.5\,{\%}
\end{align}%e13
By complement, the weighting of clear sky in layer L1 under clear sky
in layer L2 is
\begin{align}
&w^{\mathrm{L}1} ({\#}4) = 1-w^{\mathrm{L}1} ({\#}3) = 1-0.075 = 92.5\,{\%}
\end{align}%e14
Note that if \textit{cc}\,$=$\,0, or $f^{\mathrm{L}2}=1$, or
$f^{\mathrm{L}1}=1$, then $g^{\mathrm{L}1}=1$ and COR defaults to RAN. The two
additional limits on $g^{\mathrm{L}1}$ in Eq.~(10) are required to keep
$w^{\mathrm{L}1}$({\#}2) and $w^{\mathrm{L}1}$({\#}3) positive. The
$w^{\mathrm{L}2}$ weights remain simply
\begin{align}
&w^{\mathrm{L}2} ({\#}1) = w^{\mathrm{L}2} ({\#}2) = f^{\mathrm{L}2}\\
%
&w^{\mathrm{L}2} ({\#}3) = w^{\mathrm{L}2} ({\#}4) = (1-f^{\mathrm{L}2}).
\end{align}%e15 e16
The combined ICA weights are
\begin{align}

&W^{\mathrm{L}1-\mathrm{L}2} ({\#}1) = w^{\mathrm{L}1} ({\#}1) w^{\mathrm{L}2} ({\#}1) = g^{\mathrm{L}1} f^{\mathrm{L}1} f^{\mathrm{L}2} = 3 \times 0.15 \times 0.20 = 9\,{\%}\\
%
&W^{\mathrm{L}1-\mathrm{L}2} ({\#}2) = w^{\mathrm{L}1} ({\#}2) w^{\mathrm{L}2} ({\#}2) = (1-g^{\mathrm{L}1} f^{\mathrm{L}1}) f^{\mathrm{L}2} = 0.55 \times 0.20 = 11\,{\%}\\
%
&W^{\mathrm{L}1-\mathrm{L}2} ({\#}3) = w^{\mathrm{L}1} ({\#}3) w^{\mathrm{L}2} ({\#}3) = f^{\mathrm{L}1} (1-g^{\mathrm{L}1} f^{\mathrm{L}2}) = 0.15 \times 0.40 = 6\,{\%}\\
%
&W^{\mathrm{L}1-\mathrm{L}2} ({\#}4) = w^{\mathrm{L}1} ({\#}4) w^{\mathrm{L}2} ({\#}4) = 1-f^{\mathrm{L}2}-f^{\mathrm{L}1} (1-g^{\mathrm{L}1} f^{\mathrm{L}2}) = 1-0.20-0.06= 74\,{\%}
\end{align}%ee17 -- e20

As in RAN, ICAs {\#}1 and {\#}3 are tagged as cloudy in layer L1;~~,~~ and ICAs {\#}2 and {\#}4 are tagged as clear in layer L1;~~,~~ and the sum of cloudy fractions is conserved (9\,{\%}\,$+$\,6\,{\%}\,$+$\,15\,{\%}\,$=$\,$f^{\mathrm{L}1}$)~~,~~ but with different weightings. The COR model also has ICAs scaling as 2$^{\text{NL}}$.

\subsection{Maximal overlap group (MAX)}%s2.3

For maximal overlap of clouds (MAX) as in Fig.~1, the two layers L1 {and} L2 form a~MAX group G1 consisting of 1 clear-sky column (80\,{\%} fractional coverage) and 2 cloudy columns -- one with clouds in both layers (15\,{\%}) and one with a~cloud only in the upper layer L2 (5\,{\%}). For a MAX group, there can be several ICAs with cloud fractions, each with a unique combination of cloudy layers. The clear-sky column does not occur if any of the MAX layers has a~cloud fraction of 100\,{\%}. For continuous cloud fractions, the number of ICAs equals the number of ~~different~~ unique cloud fractions present (plus 1 if clear sky present). ~~,~~ If all cloud fractions are binned into the nearest 10%, then the upper limit is 10.~~and thus it scales as NL, the number of layers in the MAX group.~~ A~MAX group is characterized by the number of unique cloudy fractions (f_{1}, f_{2}, f_{3}, {\ldots}) and their weights (w_{1}, w_{2}, w_{3}, {\ldots}) with a~total cloudy fraction~~sum~~ $F = \sum f_{\mathrm{i}} \le 1$ and a~(possible) clear-sky column of fraction $1-F$. As in the earlier Fast-J work (Neu et~al., 2007), the cloud fractions in Cloud-J are quantized to limit the number of ICAs in a~MAX group. The examples here use 10\,bins, and hence cloud fractions are limited to 0, 10, 20, 30,{\ldots}, 100\,{\%}. With this binning, the in-cloud water content is scaled to conserve the cloud water content in each layer. This approximation is then resolution independent in terms of the number of model layers and limits each MAX group to 10 ICAs.

\subsection{Maximal groups with correlated overlap (MAX-COR)}%s2.4

The MAX-COR model generates ICAs from upper and lower layers that are MAX groups. For a~general approach, we ~~will~~ assume that the upper group G2 consists of N2 cloudy columns (members) with fractions $f^{\mathrm{G}2}_{\mathrm{J}2=1:\mathrm{N}2}$ totaling $F^{\mathrm{G}2}$ and 1 clear-sky column (member) of fraction

```
      $1-F^{\mathrm{G}2}$. Likewise, the lower group G1 has N1 cloudy
      members with fractions $f^{\mathrm{G}1}_{\mathrm{J}1=1:\mathrm{N}1}$
      totaling $F^{\mathrm{G}1}$ and a~clear-sky with fraction
      $1-F^{\mathrm{G}1}$. Each of the cloudy members in group G1,
      $f^{\mathrm{G}1}_{\mathrm{J}1=1:\mathrm{N}1}$, will are be paired with
      N2\,(cloudy)\,$+$\,1\,(clear) member above. The number of ICAs is the
       product will be
      (N1\,$+$\,1) (N2\,$+$\,1),
       assuming that there are clear-sky members
      in both groups. The ICA sequence (J1, J2) is then
\begin{align}
&(1,1), (2,1), (3,1), {\ldots} (\text{N}1 + 1,1), (1,2), (2,2), (3,2), {\ldots}
(\text{N}1 + 1,\text{N}2 + 1)
\end{align}%e21
      such that ICA {\#}M is composed of members
\begin{align}
&\text{J}1 = (\text{M}-1)~\text{modulo}~(\text{N}1+1) + 1\\
%
&\text{J}2 =~\text{integer}~((\text{M}-1)/(\text{N}1+1))~\text{modulo}~(\text{N}2+1)
+ 1
\end{align}%e22 e23
      The cloud correlation factor is same for all members, derived from the total
      cloudy fractions $F^{\mathrm{G}1}$ and $F^{\mathrm{G}2}$.
\begin{align}
&g^{\mathrm{G}1}  = 1 +~\text{cc}~(1/F^{\mathrm{G}2}-1),~\text{subject to}~g\le
1/F^{\mathrm{G}1}~\text{and}~g\le 1/F^{\mathrm{G}2}
\end{align}%e24
      For convenience denote J1\,$\le$\,N1 as cloudy$^{\mathrm{G}1}$,
      J1\,$=$\,N1\,$+$\,1 as clear$^{\mathrm{G}1}$, J2\,$\le$\,N2 as
      cloudy$^{\mathrm{G}2}$, and J2\,$=$\,N2\,$+$\,1 as
      clear$^{\mathrm{G}2}$. Then the weightings for the G1 members are
\begin{align}
&w^{\mathrm{G}1}
(\text{cloudy}^{\mathrm{G}1},~\text{cloudy}^{\mathrm{G}2})=g^{\mathrm{G}1}
f^{\mathrm{G}1}_{\mathrm{J}1}\\
%
&w^{\mathrm{G}1} (\text{clear}^{\mathrm{G}1},~\text{cloudy}^{\mathrm{G}2})=1-
\sum_{\text{J}1 = 1:\text{N}1} ~g^{\mathrm{G}1}  f^{\mathrm{G}1}_{\mathrm{J}1}=1-
g^{\mathrm{G}1}F^{\mathrm{G}1}
\end{align}%e25 e26
      Conserving each cloudy group member's fractional area in G1 gives the
      weights under G2 clear sky.
\begin{align}
&w^{\mathrm{G}1}
(\text{cloudy}^{\mathrm{G}1},~\text{clear}^{\mathrm{G}2})=f^{\mathrm{G}1}_{\mathrm{J}
1} (1-g^{\mathrm{G}1}  F^{\mathrm{G}2})/(1-F^{\mathrm{G}2})\\
%
&w^{\mathrm{G}1} (\text{clear}^{\mathrm{G}1},~\text{clear}^{\mathrm{G}2})=1-
F^{\mathrm{G}1} (1-g^{\mathrm{G}1} F^{\mathrm{G}2})/(1-F^{\mathrm{G}2})
\end{align}%e27 e28
      All of these formulae work also if $F^{\mathrm{G}1}>F^{\mathrm{G}2}$,
      and if $F^{\mathrm{G}1}=0$ or 1 (same for
      $F^{\mathrm{G}2}$). A~special case of MAX-COR is MAX-RAN when
      $\text{cc}=0$. With the cloud fractions binned into 10 intervals, then
      the number of ICAs for MAX-COR or MAX-RAN models scales as
      10$^{\text{NG}}$, where NG is the number of MAX groups.



\subsection{$J$~value errors}%s2.5

      Our recommended cloud overlap model uses the information on vertical
      correlations (Pincus et~al., 2005; Naud and DelGenio, 2006; Kato
```

et~al., 2010; Oreopoulis et~al., 2012), which shows cloud decorrelations
lengths of order 1.5\,\unit{km} in the lower atmosphere st layers increasing to
3\,\unit{km} or more in the upper troposphere. Since a~true COR model
will scales as 2$^{\text{NL}}$ and becomes rapidly impractical for
high-resolution models, we define vertical 6 MAX groups of cloud layers
globally
according to the as those layers within
a~decorrelation lengths: 0--1.5\,\unit{km} altitude,
1.5--3.5, 3.5--6,
6--9, 9--13, and >13\,\unit{km}.
We assume that tThe cloud layers within a decorrelation length each of these
groups are highly
correlated with
one another and thus , and we make the assumption that they form a The
MAX group.
When such MAX groups are adjacent they have a mean separation of one
decorrelation length, and
These groups collapse if there
are no cloud fractions
within the layers of the group. Each MAX group is separated by the
cloud
decorrelation length and thus we choose a~cloud correlation factor
$\text{cc}=0.33$, similar to one e-fold. When there is a clear-sky gap
between a pair of G6 layers, the MAX groups are separated by more than one
decorrelation length; thus we reduce the factor cc with successive multiples
(i.e., with 2 missing G6 MAX groups between two cloudy layers, the effective
$\text{cc}=0.33^{3} = 0.036$)., to represent the correlation of
cloudy layers between groups.
This model
is denoted G6/.33. Two other G6 models were tested: $\text{cc}=0.00$
corresponds to randomly overlapped adjacent groups (MAX-RAN, G6/.00);
and $\text{cc}=0.99$ is almost maximally overlapped (MAX, G6/.99).

In looking at
how this model aligned the clouds for realistic FCAs, we found that
extensive cirrus fractions in the uppermost layers prevented the
correlation expected overlap of small-fraction cumulus below. Thus a~7th MAX
group iwas
added if there was a~cirrus shield (defined from top down as adjacent
ice-only clouds with $f > 0.5$). We chose a~correlation factor
$\text{cc}=0.33$, similar to one e-fold, between groups, as the groups
are chosen to be separated by about one correlation length. This model
is denoted G6/.33. Two other G6 models were tested: $\text{cc}=0.00$
corresponds to MAX-RAN (G6/.00); and $\text{cc}=0.99$ is close to one
large MAX group (G6/.99). Because of the cloud-fraction binning
into 10\,{\%) intervalss and the
fixed correlation-length groups, the number of ICAs is bounded by
5×10^{6} (including the cirrus shield). This limit is
resolution independent and was never reached in any FCAs examined here
(highest number of ICAs for one FCA was 3500). The major computational
cost comes with the Fast-J computation, and the methods for
approximating the average of J~values over all ICAs (Sect.~3) use requires
at most 4 Fast-J calculations no matter how many ICAs.

Two other cloud overlap models tested here are the MAX-RAN groupings G0 and G3
,
the same or similar to earlier work (Feng et~al., 2004; Neu et~al.,
2007). The mModel G0 assumes that all vertically declares all
adjacent cloudy layers are to be a~MAX
group (maximally overlapped), and all such
groups separated by a~clear layer are to be RAN
overlapped. This model seems logical
but has difficulty finding a clear layer when the FCA has been

averaged over several hours or taken from a parameterized cloud-resolving model.
It our tests, using meteorological data with NL=36, the maximum number of G0 ICAs was 375.
Model G3 has at most 3 MAX-RAN groups demarcated by atmospheric regimes: a fixed altitude (1.5\,\unit{km}, stratus) and temperature (the liquid-to-ice cloud transition). The maximum possible number of ICAs per FCA for G3 is has the potential to be unstable with increasing layers as alternating clear and cloud layers results in 2$^{\text{NL}/2}$ ICAs. In our tests using meteorological data with NL\,$=36$, the maximum number of ICAs, 375, was well below this limit. The model G3 declares MAX groups by 3 atmospheric regimes: 0--1.5\,\unit{km} altitude as stratus-like clouds, 1.5\,\unit{km} to the uppermost mixed-phase clouds as cumulus-like clouds, and all ice-only cirrus-like clouds. With cloud-fraction bins, this model is limited to 10^{3}, \, and in our tests we found ICAs, independent of vertical resolution, and had a~maximum of 288. ICAs in our tests.

Our recommendedbest cloud overlap model is G6/.33 since it is based on the observed-modeled cloud decorrelation lengths. For a~given FCA, we treat the J~values calculated by summing Fast-J over all the ICAs generated by G6/.33 as the correct value. We calculate errors for the other cloud-overlap models (here) or various ICA-approximation models using the G6/.33 model (Sect.~3). The errors in photolysis rates are calculated for different cloud overlap models by generating all the ICAs, using Fast-J to calculate J~values, and computing the weighted sum of J's. This study focuses on two J~values that are critical in tropospheric chemistry and emphasize different wavelength ranges from near 300\,\unit{nm}, where \chem{O_3} absorption and molecular scattering are important, to 600\,\unit{nm}, where clouds are the predominant factor. J-O^{1}D refers to the photolysis rate of \chem{O_{3}}\,$+$\,$h\nu$\,$\Rightarrow$\,\chem{O_{2}}\,$+$\,O(^{1}D); and J-\chem{NO_3} includes both channels of the rate \chem{NO_{3}}\,$+$\,$h\nu$\,$\Rightarrow$\,\chem{NO}\,$+$\,\chem{O_2} and \chem{NO_{2}}\,$+$\,O. We tested other key J~values like those of \chem{HNO_3} and \chem{NO_2}, but found that their errors fell between the first two.

The J~value tests are summarized in Table~1. We use a~high-resolution snapshot from the European Center for Medium-range Weather Forecasts, similar to what is used (at lower resolution) in the UC Irvine and University of Oslo chemistry-transport models (Sovde et~al., 2012; Hsu and Prather, 2014). The 640 FCAs are a~3\,h average of a~single longitudinal belt just above the equator (T319L60 Cycle 36) and have clouds only in the lowermost 36 layers. Profiles of temperature and ozone are taken from tropical mean observations; the Rayleigh-scattering optical depth at 600\,\unit{nm} is about 0.12; and a~mix of aerosol layers has total optical depth of 0.23. J~value errors are calculated separately for each FCA and then averaged. The number of ICAs per FCA averages 169 for model G6, 21 for model G3 and 19 for model G0; see Fig.~2 for the probability distribution of ICA numbers. Errors are pressure-weighted and include the average error over 0--1\,\unit{km} altitude, the root-mean-square (rms) error over 0--1\,\unit{km}, and the full tropospheric rms error (0--16\,\unit{km}). The average 0--1\,\unit{km} differences across the models is small (< 2\,{\%}), but the rms 0--1 and 0--16 differences are large, indicating that 640 different FCAs produce canceling errors in the mean. The rms errors for G0 and G3 are worrisome, more than 15\,{\%} in the boundary layer and 5 to 11\,{\%} in the full troposphere. The G6 errors are almost linear with the \textit{cc} value. The G6/.99 with highly correlated overlap is similar to G3 which has MAX overlap throughout most of the atmosphere. The G6/.00 with random overlap is the closest to the correlated model G6/0.33.

\section{Approximating the exact sum over ICAs}%s3

Quadrature column atmospheres (QCAs) have been defined previously (Neu et~al., 2007) as 4 representative ICA-like atmospheres that represent 4 domains of ICAs with total cloud optical depths at 600\,\unit{nm} of 0 to 0.5 (clear sky), 0.5 to 4 (cirrus-like), 4 to 30 (stratus-like), and > 30 (cumulus-like). The original model sorted the ICA optical depths to get the weightings of each QCA and then picked the ICA that occurred at the mid-point in terms of fractional area (MdQCA). Thus there could 4 separate calls to Fast-J for each of the QCAs, but on average there are ~~–~~ 2.8 QCAs per FCA because not all four of the QCA ranges of cloud optical depths (0 – 0.5, 0.5 – 5, 5 – 30, >30) are present in each FCA. Here we extend that work with three new methods for approximating the integral over ICAs: define each QCA from the average ICAs in its domain (AvQCA); use the averaged direct solar beam from all ICAs to derive an effective scattering optical depth from clouds in each layer (AvDir); and, a~model with comparable computation cost to the QCAs, select 3 random ICAs based on their weights (Ran-3).

The AvQCA model comes easily from the MdQCA formalism, but all ICAs in each of the 4 total optical depth domains are used to calculate the average cloud-water content in each QCA. The AvDir model calculates the weighted direct solar beam from each ICA, where only 600\,nm cloud extinction is included. In this case it was found that an equivalent isotropic extinction is needed as in two-stream methods (Joseph et~al., 1976), and we scaled the optical depth of each cloud layer by a~factor: 1--1.1\,$\times$\,P$_{1}/3$, with a~minimum value of 0.04. P$_{1}$ (3 times the asymmetry factor) is the second term in the Legendre expansion of the scattering phase function for the cloud in that layer. The derived optical depth in each layer is calculated from the reduction in direct beam across the layer (Beer--Lambert Law) and put into the single Fast-J calculation with the original cloud properties of that layer, not the equivalent isotropic properties.

In addition to these ICA approximations, we also compare the G6/.33 exact sum over ICAs with three simple cloud models often use in chemistry models that do not generate ICAs: clear sky (ClSky); averaged cloud over each layer (AvCld); and cloud fraction to the 3/2 ($f^{3/2}$, CF3/2).

A~sample of mean and rms errors for the seven approximate methods is given in Table~1. In addition, a~tropospheric profile of the mean bias in J~values is shown is Fig.~3. As expected the ClSky and AvCld methods show opposite biases and large RMS errors. The CF3/2 method produces reasonable averages, but still has rms errors of 10\,{\%} or more. The AvDir method ~~did~~ does not perform as well as expected and looks only slightly better than CF3/2; however, the profile of mean error (Fig.~3) is preferable to that of CF3/2. Both QCA methods performed excellently and deliver rms errors less than 5\,{\%} with mean biases in the boundary layer of order $\pm$1\,{\%}. The new AvQCA method has smaller rms errors for the cases in Table~1, but the original MdQCA method may have a~better profile for the mean error. Ran-3 is computationally comparable to the QCAs and has a~reasonable mean bias, but the rms error is much worse, typically 10\,{\%} more.

\section{Cloud-J and volatile organic compounds}%s4

Volatile organic compounds (VOCs) cover a~wide class of gaseous species containing C, H, O and sometimes N or S. They play a~major role in the chemical reactivity of the troposphere, including production and loss of \chem{O_3} and loss of \chem{CH_4} (e.g., Jacob et~al., 1993; Horowitz et~al., 1998; Ito et~al., 2009; Emmons et~al., 2010), plus the formation of secondary organic aerosols (SOA, e.g., Ito et~al., 2007; Fu et~al., 2008; Galloway et~al., 2011). For most VOCs (and \chem{H_2O_2}) photolysis is the dominant loss, see Fig.~4. Daily photolysis rates (loss frequencies) range from 0.03 to 20 per day and some vary greatly with altitude. For 9 of the 14 species shown in Fig.~4, the photolysis rates are larger or comparable to the loss rates for reaction with OH (given in the legend). Thus, accurate calculation of their J~values is important in atmospheric chemistry models.

VOCs present a~particular problem for any photolysis code that averages over wavelength intervals. For most chemical species, cross sections including quantum yields are parameterized as a~function of wavelength (v) and temperature (T) (e.g., Atkinson et~al., 2008; Sander et~al., 2011). In this case, Fast-J calculates solar-flux-weighted, average cross sections for each wavelength bin (Wild et~al., 2000; Bian and Prather, 2002). These tables are created for a~set of fixed Ts, and then the cross section used for each bin in each atmospheric layer is interpolated in T. Many VOCs have complex, pressure-dependent quantum yields (e.g., Blitz et~al., 2006) that follow the Stern--Volmer formulation where photolysis cross sections (for dissociation) are a~function of wavelength, temperature, and pressure (P), typically of the form
$A(T,v)/(1+B(T,v)P)$,
where A and B can be rational polynomial functions of T and v (see Sander et~al., 2011). For most VOCs the pressure dependence changes across the wavelengths within a~model bin, and thus the T dependence averaged cross sections ~~will have~~ has different values at different P, but cannot be simply post-interpolated as a~function of P because of the wavelength dependence of B. A~two-dimensional set of cross sections for each wavelength bin, interpolated as a~function of T and P, could be developed but would add to the complexity and cost of Fast-J.

Recognizing that VOCs are predominantly tropospheric and that T and P are highly correlated in the troposphere, Cloud-J, and the new Fast-J that sits within it, have devised an alternative method of interpolating the cross sections for each atmospheric layer: T is the traditional method used for most species; but P is used for VOCs with highly pressure-dependent quantum yields. For P interpolation, the cross sections are averaged over wavelength at 3 points along a~typical tropospheric lapse rate: (0\,\unit{km}, 295\,\unit{K}, 999\,\unit{hPa}); (5\,\unit{km}, 272\,\unit{K}, 566\,\unit{hPa}); and (13\,\unit{km}, 220\,\unit{K}, 177\,\unit{hPa}). Currently species with P interpolation include: acetaldhyde, methylvinyl ketone, methylethyl ketone, glyoxal, methyl glyoxal, and one branch of acetone photolysis. Fast-J does not extrapolate beyond its supplied tables, and thus currently it applies 177\,hPa cross sections for these VOCs throughout the stratosphere, but this ~~should~~ has ~~have~~ minimal impact on stratospheric chemistry. Depending on the available laboratory data, the number of cross-section tables per species in the new Fast-J (either T or P interpolation) can be 1, 2, or 3. Cloud-J, new with version 7.3, includes an updated version of Fast-J version 7.1, whose only change is in the formatting of the input files to allow for more flexible numbering and labeling of species with their cross sections and of the cloud-aerosol scattering tables.

\conclusions[Discussion and recommendations]%s5

We recommend use of the G6/.33 MAX-COR model for cloud overlap with AvQCA to approximate the average photolysis rates over the ICAs. This combination of algorithms best matches the exact solution for average J~values. Averaging J~values for an air parcel that includes a~mix of cloudy and clear air is not the same as averaging the chemical reactivity across cloudy and clear. Nevertheless, for species with photolysis rates that are less than the frequency at which clouds form and air is processed through them ($\sim 24\,\unit{day^{-1}}$), the average J is the relevant quantity for chemistry modeling.

~~The~~ A next step would be to model at high-enough resolution so that air parcels are either cloudy or clear. This could resolve the 3-D correlation of clouds at scales of 1--4\,\unit{km}, which will~~would~~ in turn require a~3-D radiative transfer model (Norris et~al., 2008; Davis and Marshak, 2010). A~more interesting approach that is practical with typical global model resolution is the treatment of inhomogeneous cloud fields as being composed of independently scattering cloudlets (Petty, 2002). This cloudlet approximation could be readily integrated into the plane-parallel framework of Fast-J.

The added computational cost with G6/.33$+$AvQCA occurs with the additional calls to Fast-J, as the MAX-COR model and sorting of ICAs is fast. Computing photolysis rates 2.8 times per atmospheric column instead of once may add to the overall computational burden, but Fast-J is efficient and the costs will ~~should still~~ be much less than the overall chemistry-solver and tracer-transport codes.

\section*{Code availability}

The most recent version of Cloud-J and earlier versions of Fast-J can be found at \url{ftp://128.200.14.8/public/prather/F~~f~~ast-J~~X~~/}. Cloud-J 7.3c~~b~~ as described here is included as a~zip-file ~~with the supplementary material of this publication.~~ and includes new coding to correct failures in compilation or execution (v7.3b) as well as reducing the cloud correlation factor when there are decorrelation-length gaps between any of the MAX-COR groups (v7.3c). Although with v7.3c some J-values changed in the third decimal place, changes in the GMDD ~~The~~ figures and tables were undiscernible. ~~remain unchanged with version 7.3b.~~
Subscribe to the listserv~~maillist~~ {UCI-Fast-J@uci.edu} or check the ftp site for updates~~ on cross sections~~. ~~following new evaluations of photochemical data.~~Send questions or suggestions for Cloud-J features to the listserv or the author (mprather@uci.edu).

\Supplementary{zip}

\begin{acknowledgements}
Research at UCI was supported by NASA grant NNX13AL12G and DOE BER award

DE-SC0012536. The author is indebted to T. Reddmann, R. Sander and an
anonymous reviewer for finding the coding inconsistencies/errors,
and Cloud-J should now be more reliable across platforms.
\end{acknowledgements}

\begin{thebibliography}{28}

\bibitem{1}
Atkinson,~R., Baulch,~D.~L., Cox,~R.~A., Crowley,~J.~N., Hampson,~R.~F.,
Hynes,~R.~G., Jenkin,~M.~E., Rossi,~M.~J., Troe,~J., and Wallington,~T.~J.:
Evaluated kinetic and photochemical data for atmospheric chemistry: Volume IV
-- gas phase reactions of organic halogen species, Atmos. Chem. Phys., 8,
4141--4496,
doi:\href{http://dx.doi.org/10.5194/acp-8-4141-2008}{10.5194/acp-8-4141-2008},
2008.

\bibitem{2}
Bian,~H.~S. and Prather,~M.~J.:
Fast-J2: accurate simulation of stratospheric photolysis in global chemical models,
J.~Atmos. Chem.,
41, 281--296, 2002.

\bibitem{3}
Blitz,~M.~A., Heard,~D.~E., and Pilling,~M.~J.: Study of acetone
photodissociation over the wavelength range 248--330\,\unit{nm}: evidence of
a~mechanism involving both the singlet and triplet excited states, J.~Phys.
Chem.~A, 110, 6742--6756,
doi:\href{http://dx.doi.org/10.1021/Jp056276g}{10.1021/Jp056276g}, 2006.

\bibitem{4}
Briegleb,~B.~P.:
Delta-Eddington Approximation for solar-radiation in the NCAR Community Climate
Model,
J.~Geophys. Res.,
97, 7603--7612, 1992.

\bibitem{5}
Davis,~A.~B. and Marshak,~A.:
Solar radiation transport in the cloudy atmosphere: a~3-D perspective on observations
and climate impacts,
Rep. Prog. Phys.,
73, 026801,
doi:\href{http://dx.doi.org/10.1088/0034-4885/73/2/026801}{10.1088/0034-4885/73/2/026801}, 2010.

\bibitem{6}
Emmons,~L.~K., Apel,~E.~C., Lamarque,~J.-F., Hess,~P.~G., Avery,~M.,
Blake,~D., Brune,~W., Campos,~T., Crawford,~J., DeCarlo,~P.~F., Hall,~S.,
Heikes,~B., Holloway,~J., Jimenez,~J.~L., Knapp,~D.~J., Kok,~G.,
Mena-Carrasco,~M., Olson,~J., O'Sullivan,~D., Sachse,~G., Walega,~J.,
Weibring,~P., Weinheimer,~A., and Wiedinmyer,~C.: Impact of Mexico City
emissions on regional air quality from MOZART-4 simulations, Atmos. Chem.

Phys., 10, 6195--6212,
doi:\href{http://dx.doi.org/10.5194/acp-10-6195-2010}{10.5194/acp-10-6195-2010},
2010.

\bibitem{7}
Feng,~Y., Penner,~J.~E., Sillman,~S., and Liu,~X.:
Effects of cloud overlap in photochemical models,
J.~Geophys. Res.,
109, D04310,
doi:\href{http://dx.doi.org/10.1029/2003JD004040}{10.1029/2003JD004040}, 2004.

\bibitem{8}
Fu,~T.~M., Jacob,~D.~J., Wittrock,~F., Burrows,~J.~P., Vrekoussis,~M., and
Henze,~D.~K.:
Global budgets of atmospheric glyoxal and methylglyoxal, and implications for
formation of secondary organic aerosols,
J.~Geophys. Res.,
113, D15303,
doi:\href{http://dx.doi.org/10.1029/2007JD009505}{10.1029/2007JD009505}, 2008.

\bibitem{9}
Galloway,~M.~M., Loza,~C.~L., Chhabra,~P.~S., Chan,~A.~W.~H., Yee,~L.~D.,
Seinfeld,~J.~H., and Keutsch,~F.~N.:
Analysis of photochemical and dark glyoxal uptake: implications for SOA formation,
Geophys. Res. Lett.,
38, L17811,
doi:\href{http://dx.doi.org/10.1029/2011GL048514}{10.1029/2011GL048514}, 2011.

\bibitem{10}
Horowitz,~L.~W., Liang,~J.~Y., Gardner,~G.~M., and Jacob, D.~J.:
Export of reactive nitrogen from North America during summertime: sensitivity to
hydrocarbon chemistry,
J.~Geophys. Res.,
103, 13451--13476, 1998.

\bibitem{11}
Hsu,~J.~N. and Prather,~M.~J.:
Is the residual vertical velocity a~good proxy for stratosphere--troposphere exchange
of ozone?,
Geophys. Res. Lett.,
41, 9024--9032,
doi:\href{http://dx.doi.org/10.1002/2014gl061994}{10.1002/2014gl061994}, 2014.

\bibitem{12}
Ito,~A., Sillman,~S., and Penner,~J.~E.:
Effects of additional nonmethane volatile organic compounds, organic nitrates, and
direct emissions of oxygenated organic species on global tropospheric chemistry,
J.~Geophys. Res.,
112, D06309,
doi:\href{http://dx.doi.org/10.1029/2005JD006556}{10.1029/2005JD006556}, 2007.

\bibitem{13}
Ito,~A., Sillman,~S., and Penner,~J.~E.:

Global chemical transport model study of ozone response to changes in chemical kinetics and biogenic volatile organic compounds emissions due to increasing temperatures: sensitivities to isoprene nitrate chemistry and grid resolution,
J.~Geophys. Res.,
114, D09301,
doi:\href{http://dx.doi.org/10.1029/2008jd011254}{10.1029/2008jd011254}, 2009.

\bibitem{14}
Jacob,~D.~J., Logan,~J.~A., Yevich,~R.~M., Gardner,~G.~M., Spivakovsky,~C.~M., Wofsy,~S.~C., Munger,~J.~W., Sillman,~S., Prather,~M.~J., Rodgers,~M.~O., Westberg,~H., and Zimmerman,~P.~R.:
Simulation of summertime ozone over North-America,
J.~Geophys. Res.,
98, 14797--14816, 1993.

\bibitem{15}
Joseph,~J.~H., Wiscombe,~W.~J., and Weinman,~J.~A.: Delta-Eddington Approximation for radiative flux-transfer, J.~Atmos. Sci., 33, 2452--2459, 1976.

\bibitem{16}
Kato,~S., Sun-Mack,~S., Miller,~W.~F., Rose,~F.~G., Chen,~Y., Minnis,~P., and Wielicki,~B.~A.:
Relationships among cloud occurrence frequency, overlap, and effective thickness derived from CALIPSO and CloudSat merged cloud vertical profiles,
J.~Geophys. Res.,
115, D00H28,
doi:\href{http://dx.doi.org/10.1029/2009JD012277}{10.1029/2009JD012277}, 2010.

\bibitem{17}
Naud,~C. and DelGenio,~A.~D.: Cloud Overlap Dependence on Atmospheric Dynamics, Sixteenth ARM Science Team Meeting Proceedings, 27--31~March 2006, Albuquerque, NM, 2006.

\bibitem{18}
Neu,~J.~L., Prather,~M.~J., and Penner,~J.~E.:
Global atmospheric chemistry: integrating over fractional cloud cover,
J.~Geophys. Res.,
112, D11306,
doi:\href{http://dx.doi.org/10.1029/2006JD008007}{10.1029/2006JD008007}, 2007.

\bibitem{19}
Norris,~P.~M., Oreopoulos,~L., Hou,~A.~Y., Taod,~W.-K., and Zenga,~X.:
Representation of 3-D heterogeneous cloud fields using copulas: theory for water clouds,
Q.~J. Roy. Meteor. Soc.,
134, 1843--1864, 2008.

\bibitem{20}
Oreopoulos,~L., Lee,~D., Sud,~Y.~C., and Suarez,~M.~J.: Radiative impacts of cloud heterogeneity and overlap in an atmospheric General Circulation Model,
Atmos. Chem. Phys., 12, 9097--9111,
doi:\href{http://dx.doi.org/10.5194/acp-12-9097-2012}{10.5194/acp-12-9097-2012}, 2012.

\bibitem{21}
Petty,~G.~W.: Area-average solar radiative transfer in three-dimensionally inhomogeneous clouds: the Independently Scattering Cloudlet Model, J.~Atmos. Sci., 59, 2910--2929, 2002.

\bibitem{22}
Pincus,~R., Hannay,~C., Klein,~S.~A., Xu,~K.-M., and Hemler,~R.:
Overlap assumptions for assumed probability distribution function cloud schemes in large-scale models,
J.~Geophys. Res.,
110, D15S09,
doi:\href{http://dx.doi.org/10.1029/2004JD005100}{10.1029/2004JD005100}, 2005.

\bibitem{23}
Sander,~S.~P., Friedl,~R.~R., Abbatt,~J.~P.~D., Barker,~J.~R., Burkholder,~J.~B., Golden,~D.~M., Kolb,~C.~E., Kurylo,~M.~J., Moortgat,~G.~K., Wine,~P.~H., Huie,~R.~E., and Orkin,~V.~L.: Chemical Kinetics and Photochemical Data for Use in Atmospheric Studies, Evaluation No. 17, Jet Propulsion Laboratory, Pasadena, CA, 2011.

\bibitem{24}
Slobodda,~J., H\"{u}nerbein,~A., Lindstrot,~R., Preusker,~R., Ebell,~K., and Fischer,~J.: Multichannel analysis of correlation length of SEVIRI images around ground-based cloud observatories to determine their representativeness, Atmos. Meas. Tech., 8, 567--578,
doi:\href{http://dx.doi.org/10.5194/amt-8-567-2015}{10.5194/amt-8-567-2015},
2015.

\bibitem{25}
S{\o}vde,~O.~A., Prather,~M.~J., Isaksen,~I.~S.~A., Berntsen,~T.~K., Stordal,~F., Zhu,~X., Holmes,~C.~D., and Hsu,~J.: The chemical transport model Oslo CTM3, Geosci. Model Dev., 5, 1441--1469,
doi:\href{http://dx.doi.org/10.5194/gmd-5-1441-2012}{10.5194/gmd-5-1441-2012},
2012.

\bibitem{26}
Stamnes,~K., Tsay,~S.~C., Wiscombe,~W., and Jayaweera,~K.: Numerically stable algorithm for discrete-ordinate-method radiative-transfer in multiple-scattering and emitting layered media, Appl. Optics, 27, 2502--2509, 1988.

\bibitem{27}
Tie,~X.~X., Madronich,~S., Walters,~S., Zhang,~R.~Y., Rasch,~P., and Collins,~W.: Effect of clouds on photolysis and oxidants in the troposphere, J.~Geophys. Res., 108, 4642,
doi:\href{http://dx.doi.org/10.1029/2003jd003659}{10.1029/2003jd003659},
2003.

\bibitem{28}
Wild,~O., Zhu,~X., and Prather,~M.~J.:

Fast-J: accurate simulation of in- and below-cloud photolysis in tropospheric
chemical models,
J.~Atmos. Chem.,
37, 245--282, 2000.

```
\end{thebibliography}


%T1
\begin{table}[t]
\caption{Models for cloud overlap and approximation of ICAs including errors in
$J$~values.}
\scalebox{.75}[.75]{%
\begin{tabular}{lp{55mm}lllcllcll}
\tophline \multicolumn{2}{l}{Cloud overlap models to generate ICAs}&
ICAs$^{\mathrm{a}}$& \multicolumn{2}{c}{avg err 0--1\,\unit{km}} &&
\multicolumn{2}{c}{rms err 0--1\,\unit{km}} &&
\multicolumn{2}{c}{rms err 0--16\,\unit{km}}\\
\cline{4-5} \cline{7-8} \cline{10-11}
\multicolumn{2}{l}{~}& & J-O$^{1}$D&J-\chem{NO_3}&&
J-O$^{1}$D&J-\chem{NO_3}&&
J-O$^{1}$D&J-\chem{NO_3}\\
\middlehline
G0&{MAX-RAN with MAX groups\par bounded by layers with CF\,$=0$}
&19&$+2\,{\%}$&$+2\,{\%}$&&21\,{\%}&17\,{\%}&&6\,{\%}&11\,{\%} \\

G3&{3 MAX-RAN groups split at 1\,\unit{km}\par and at the ice-only cloud level}
&21&$+2\,{\%}$&$+2\,{\%}$&&15\,{\%}&15\,{\%}&&5\,{\%}&7\,{\%} \\

G6/.00&{6 MAX-COR groups, cc\,$=0.00$} &169&$-$1\,{\%}&$-
$1\,{\%}&&5\,{\%}&4\,{\%}&&2\,{\%}&3\,{\%} \\

G6/.33&{6 MAX-COR groups, cc\,$=0.33^{\mathrm{b}}$} &169& & && & && & \\

G6/.99&{6 MAX-COR groups, cc\,$=0.99$}
&169&$+2\,{\%}$&$+1\,{\%}$&&11\,{\%}&8\,{\%}&&4\,{\%}&7\,{\%} \\[12pt]
\cline{1-11}
\multicolumn{2}{l}{Simple cloud models} &
ICAs&
&&&&&&&&\\
\cline{1-11}
{ClSky} &clear sky, ignore
clouds&1&$+14\,{\%}$&$+10\,{\%}$&&24\,{\%}&20\,{\%}&&14\,{\%}&23\,{\%} \\

{AvCld} &average fractional cloud across\par layer&1&$-
$5\,{\%}&$+1\,{\%}$&&11\,{\%}&11\,{\%}&&8\,{\%}&15\,{\%} \\

{CF3/2} &increase CF to CF$^{3/2}$ and average\par over
layer&1&$+7\,{\%}$&$+11\,{\%}$&&10\,{\%}&15\,{\%}&&5\,{\%}&8\,{\%} \\[12pt]
\cline{1-11}
\multicolumn{2}{l}{ICA approximations} &
J calls&
&&&&&&&&\\
\cline{1-11}
{AvDir} &average direct beam from all
ICAs&1&$+5\,{\%}$&$+11\,{\%}$&&6\,{\%}&13\,{\%}&&3\,{\%}&7\,{\%} \\

{MdQCA} &Quadrature Column Atmospheres\par uses mid-point in each
QCA&2.8&$+1\,{\%}$&0\,{\%}&&4\,{\%}&4\,{\%}&&4\,{\%}&5\,{\%} \\

{AvQCA} &QCAs, uses average in each QCA&2.8&$-
$1\,{\%}&0\,{\%}&&3\,{\%}&2\,{\%}&&2\,{\%}&4\,{\%} \\
```

```
{Ran-3} &Select 3 ICAs at
random&3&$+2\,{\%}$&$+1\,{\%}$&&12\,{\%}&12\,{\%}&&9\,{\%}&12\,{\%} \\
\bottomhline
\end{tabular}
} \scalebox{.75}[.75]{
\belowtable{%
\hack{\vspace*{2mm}}
$^{\mathrm{a}}$ Average number of ICAs for a tropical atmosphere, see Fig. 2. \\
$^{\mathrm{b}}$ Recommended cloud overlap model and reference model for calculation
of errors. \\
}
}
\end{table}


\begin{figure}
\includegraphics[width=120mm]{gmd-2015-82-discussions-f01.pdf}
\caption{Schematic of overlapping fractional-cloud layers. See text.}
\label{gmdd-2015-0082-f01.pdf}
\end{figure}


\begin{figure}
\includegraphics[width=120mm]{gmd-2015-82-discussions-f02.pdf}
\caption{Number of Independent Column Atmospheres (ICAs) generated by three different
cloud overlap models (G0, G3, G6) from 640 different tropical fractionally cloudy
atmospheres (FCAs) and sorted in order of increasing ICA number. The different cloud
correlation coefficients factors used in the G6 model do not change the number of
ICAs, only their weights. The average number of ICAs per FCA is given in the legend.
See text for definition of models.}
\label{gmdd-2015-0082-f03.pdf}
\end{figure}


\begin{figure}
\includegraphics[width=120mm]{gmd-2015-82-discussions-f03.pdf}
\caption{Profile of the average bias in $J$~value approximations relative to the
$J$~value calculated from the weighted average of all ICAs using model G6/.33. Values
here are calculated using a solar zenith angle of 13.6~degrees and a surface albedo
of 0.10 and the averaged overof 640 FCAs (108,125 ICAs) derived from the equatorial
statistics (all longitudes) of cloud fraction, liquid water content, and ice water
content from a~snapshot of a~T319L60 meteorology from the European Centre for Medium-
range Weather Forecasts. Three simple cloud methods (dashed lines) do not use any
cloud-overlap model, and three approximations for the ICAs (solid lines) use the
G6/.33 model described here. The MdQCA ICA approximation was developed in Neu
et~al.~(2007); the AvQCA and AvDir approximations are developed in this paper. The J-
O$^1$D refers to the photolysis rate of
\chem{O_{3}}\,$+$\,$h\nu$\,$\Rightarrow$\,\chem{O_{2}}\,$+$\,O($^{1}$D), with average
values of 4 ($z=0$\,\unit{km}) to 9 ($z=16$\,\unit{km})\,$\times$\,10$^{-
5}$\,\unit{s^{-1}}; and J-\chem{NO_3}, to all channels of the rate
\chem{NO_{3}}\,$+$\,$h\nu$\,$\Rightarrow$, with average values of 2 to $4 \times
10^{-1}$\,\unit{s^{-1}}. These two $J$~values emphasize sunlight from 310 to
600\,\unit{nm}, respectively, and thus span the typical range of errors in
tropospheric photolysis rates.}
\label{gmdd-2015-0082-f05.pdf}
\end{figure}

\begin{figure}
\includegraphics[width=70mm]{gmd-2015-82-discussions-f04.pdf}
\caption{Volatile organic compounds (VOCs) and related species photolysis rates
(\unit{day^{-1}}) as a~function of altitude (km). The complex structure with altitude
is due to  a~combination of increasing UV-radiation with altitude and Sterm--Volmer
pressure dependences on quantum yields. Changes in slope occur at the interpolation
```

```latex
points, temperature or pressure, of the cross sections. We assume that the noon-time
$J$'s (clear-sky, tropical atmosphere, albedo\,$=$\,0.10, SZA\,$=$\,15{\degree})
apply for 8 of 24\,h. Equivalent rates for OH loss are shown with the species name in
the legend and assume a~noontime OH density of 6\,$\times$\,10$^{6}$\,\unit{cm^{-3}}.
Asterisks denote species for which photolysis loss is greater than or comparable to
OH loss. VOC abbreviations are: MGlyxl\,$=$\,methyl glyoxal; Glyxl\,$=$\,glyoxal;
PropAld\,$=$\,propionaldehyde; GlyAld\,$=$\,glycol aldehyde;
ActAld\,$=$\,acetaldehyde; MEKeto\,$=$\,methylethyl ketone; MeVK\,$=$\,methylvinyl
ketone; MeOOH\,$=$\,\chem{CH_3OOH}; MeAcr\,$=$\,methacrolein;
\chem{MeNO_3}\,$=$\,methyl nitrate; PAN\,$=$\,peroxyacetyl nitrate.}
\label{gmdd-2015-0082-f06.pdf}
\end{figure}



\end{document}
\endinput
```

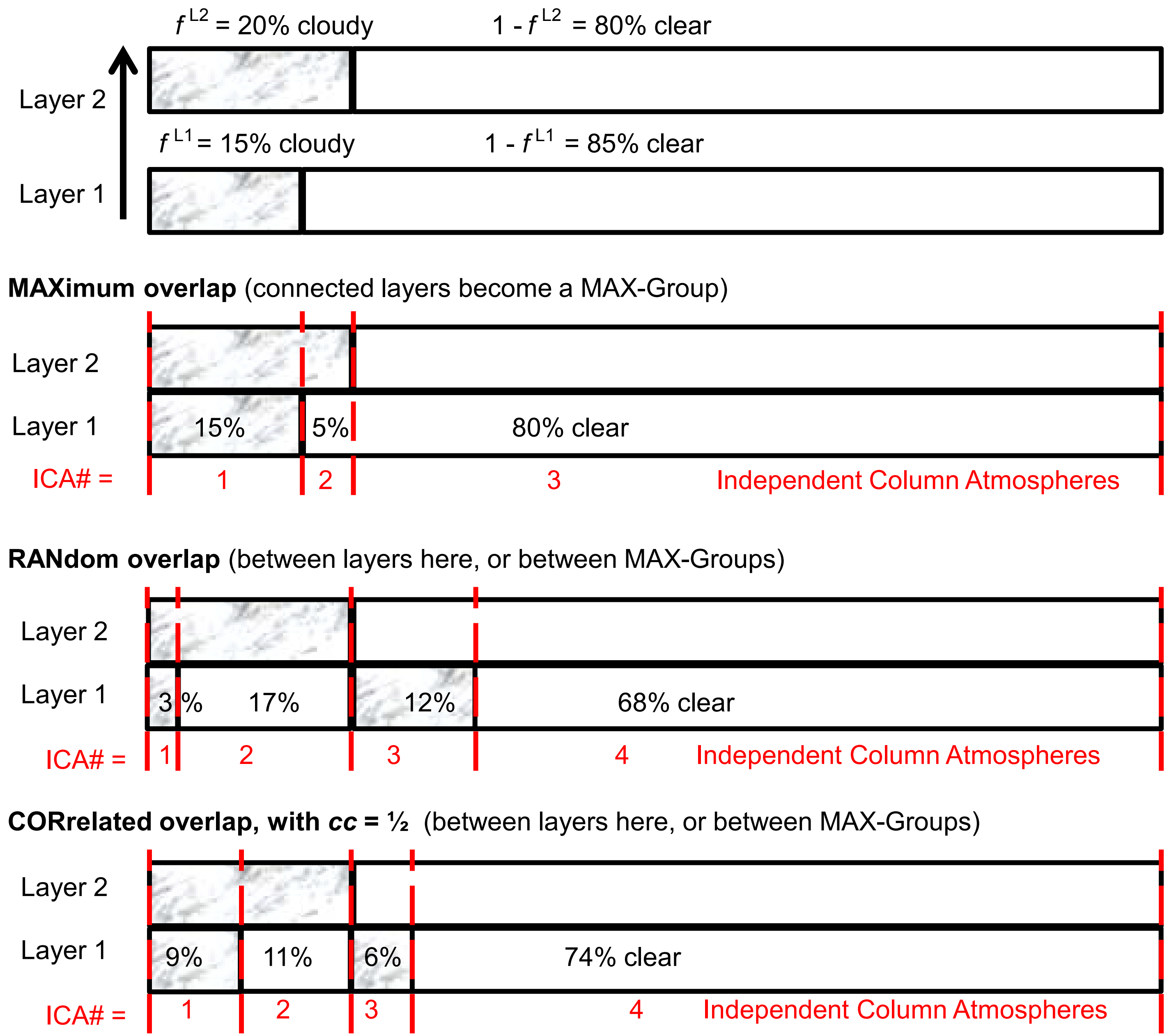

f L2 = 20% cloudy
1 - f L2 = 80% clear
Layer 2
f L1 = 15% cloudy
1 - f L1 = 85% clear
Layer 1
MAXimum overlap (connected layers become a MAX-Group)
Layer 2
Layer 1
15%
5%
80% clear
ICA# =
1
2
3
Independent Column Atmospheres
RANdom overlap (between layers here, or between MAX-Groups)
Layer 2
Layer 1
3%
17%
12%
68% clear
ICA# =
1
2
3
4
Independent Column Atmospheres
CORrelated overlap, with cc = ½ (between layers here, or between MAX-Groups)
Layer 2
Layer 1
9%
11%
6%
74% clear
ICA# =
1
2
3
4
Independent Column Atmospheres

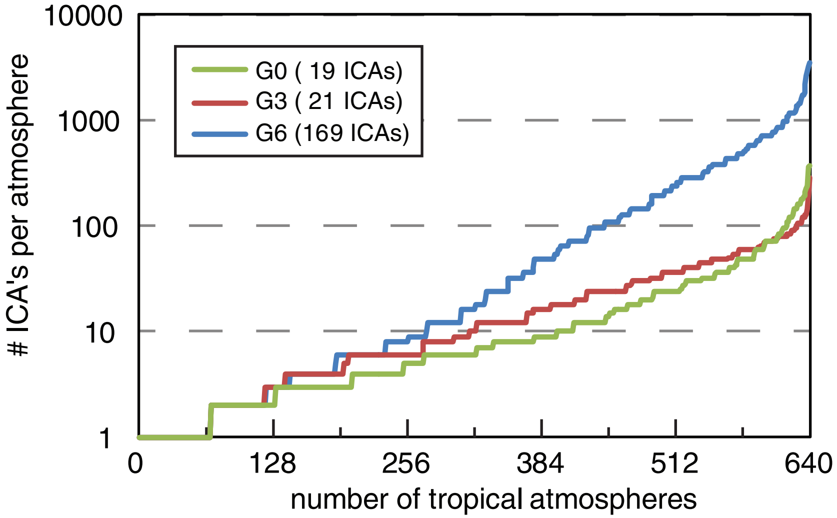

G0 (19 ICAs)
G3 (21 ICAs)
G6 (169 ICAs)
10000
1000
100
10
1
0
128
256
384
512
640
ICA's per atmosphere
number of tropical atmospheres

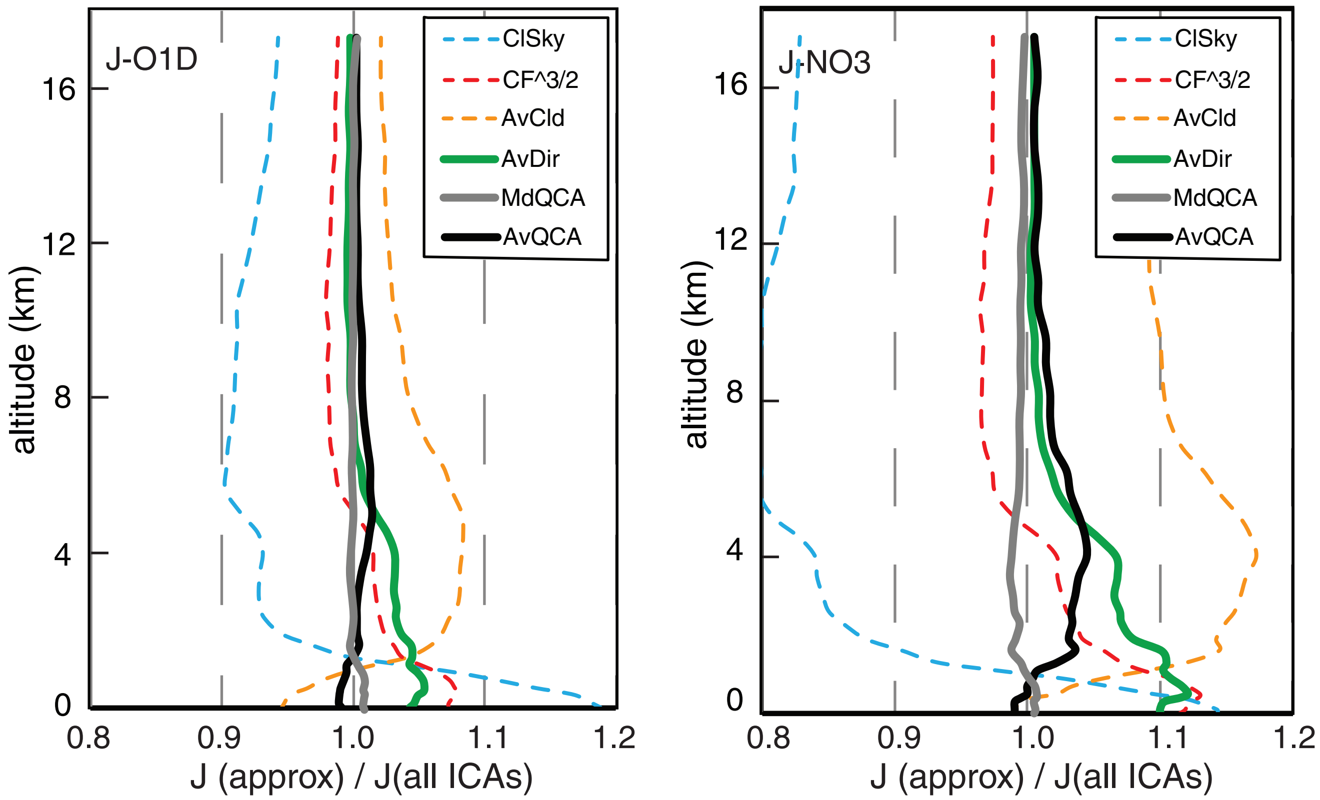
J-O1D
ClSky
CF^3/2
AvCld
AvDir
MdQCA
AvQCA
altitude (km)
0
4
8
12
16
0.8
0.9
1.0
1.1
1.2
J (approx) / J(all ICAs)
J-NO3
ClSky
CF^3/2
AvCld
AvDir
MdQCA
AvQCA
altitude (km)
0
4
8
12
16
0.8
0.9
1.0
1.1
1.2
J (approx) / J(all ICAs)

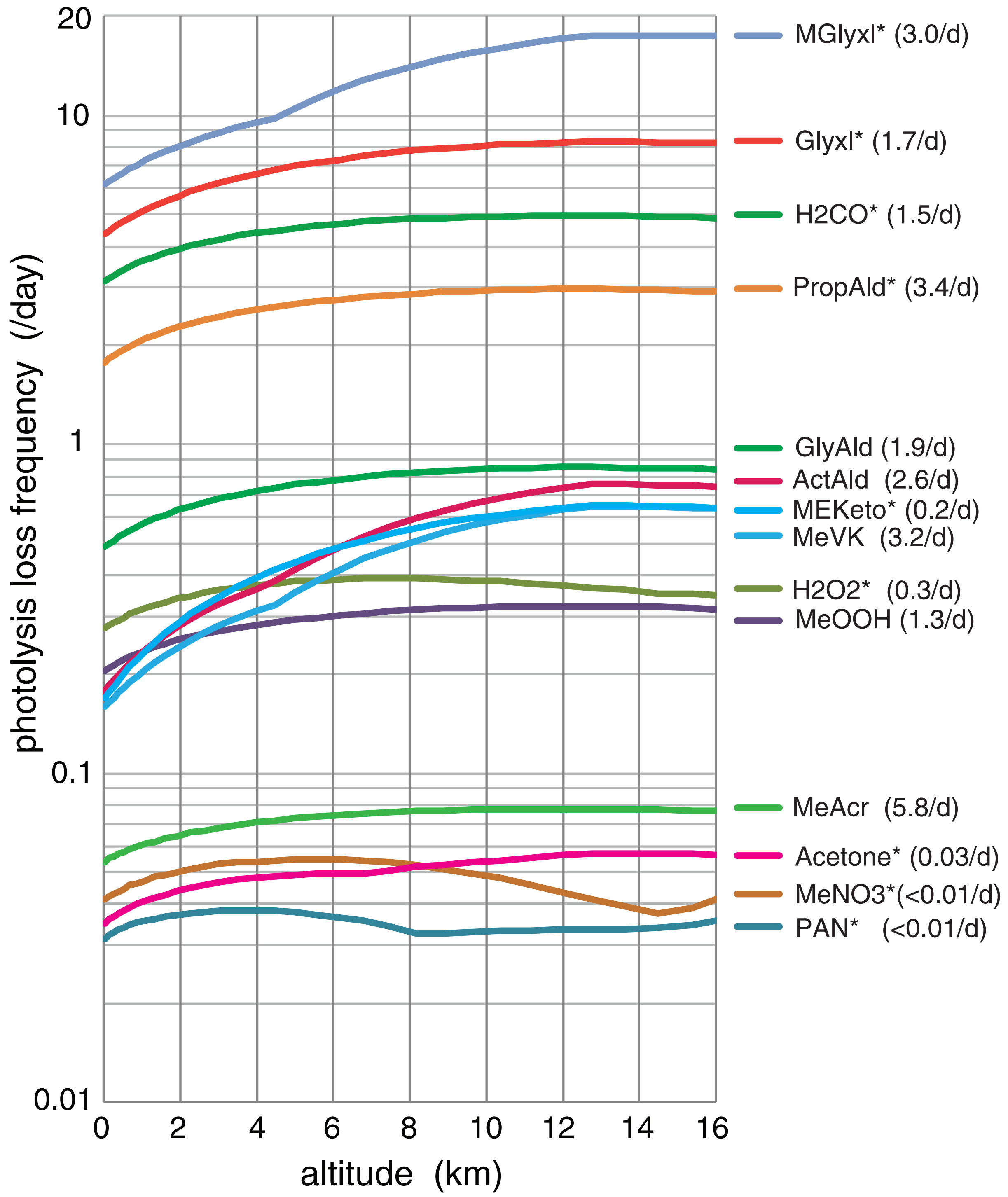

20
10
1
0.1
0.01
photolysis loss frequency (/day)
0
2
4
6
8
10
12
14
16
altitude (km)
MGlyxl* (3.0/d)
Glyxl* (1.7/d)
H2CO* (1.5/d)
PropAld* (3.4/d)
GlyAld (1.9/d)
ActAld (2.6/d)
MEKeto* (0.2/d)
MeVK (3.2/d)
H2O2* (0.3/d)
MeOOH (1.3/d)
MeAcr (5.8/d)
Acetone* (0.03/d)
MeNO3*(<0.01/d)
PAN* (<0.01/d)